# Microencapsulation of isocyanate compounds for autoreactive, monocomponent adhesive

**Mahboobeh Attaei**

mahboobehattaei@tecnico.ulisboa.pt
*Instituto Superior Técnico, Universidade de Lisboa*

ARTICLE INFO

Article date:
October,2017

*Keywords:*
*Microencapsulation; Interfacial polymerization; Adhesive material; Isocyanate*

ABSTRACT

The present paper regards the microencapsulation of toxic isocyanate, used as a crosslinker in adhesive formulations, for the footwear industry with the idea of reducing the risk of its handling and enabling mono-component formulations. Micro emulsion technique combined with interfacial polymerization was the approach selected to produce microcapsules (MCs), with a shell of polyurea (PUa) and/or polyurethane (PU) containing different isocyanate compounds in their core, e.g. isophorone diisocyanate (IPDI), toluene diisocyanate (TDI) and mixtures of monomeric and polymeric species of methylene diphenyl diisocyanate (MDI).
Fourier transformed infrared spectroscopy (FTIR) and thermogravimetric analysis (TGA) were employed to characterize the MCs concerning the presence of free -NCO groups and, therefore, the success of the isocyanate encapsulation. Scanning electron microscopy (SEM) was used to study the morphology of the MCs, i.e. to check if they exhibit a core-shell structure. Several studies were carried out in order to understand the effect of the different synthesis parameters e.g., temperature, stirring rate and quantity of surfactant, on the shape and size of the MCs, as well as on the encapsulation efficiency of isocyanate compounds Moreover, a series of reagents and polymers were added to the syntheses with the aim of changing the morphology and properties of the MCs shell. Finally, peeling strength tests were carried out at different conditions of temperature and pressure, in order to study the failure type of the adhesive joint, which depends on the interaction of the MCs with the base adhesive component (OH-rich), as well as on the isocyanate release from the MCs and is an indication of the adhesion efficiency.

## 1.Introduction

High quality, strong and long-lasting adhesives used in the footwear, automobile and aerospace industries are typically isocyanate-based in order to provide high strength joints. These adhesives are supplied in two components, one being isocyanate and the other being polyol based, to be mixed at a certain proportion by the user. High toxicity of isocyanate-based compounds is restricting their use in the industry, based on current legislation. Companies in the adhesive sector, such as CIPADE S.A. (with whom IST has a partnership in the framework of a Portugal 2020 Co-Promotion project, ECOBOND) are, therefore, willing to offer a safe adhesive solution to these

industries, but still based on isocyanate chemistry due to its high adhesive efficiency (ECOBOND, 2015). The isocyanate chemical group is extremely reactive, forming a chemical bond with any chemical group that contains an active hydrogen atom, i.e. primary and secondary hydroxyl groups, aliphatic and aromatic amines, primary and tertiary hydroxides, urea and urethane proton, among others (Langenberg, 2010). Generally, isocyanate compounds with two NCO groups per molecule are used to produce isocyanate-based adhesives. The two most important diisocyanates are methylene diphenyl diisocyanate (MDI) and toluene diisocyanate (TDI) and their reaction with polyols can lead to a large number of adhesive systems and formulations, due to the isocyanate group's chemical reactivity (Langenberg, 2010).

Microencapsulation of isocyanate compounds may occur by formation of PUa or PU shell by reaction between isocyanate and active hydrogen sources at the interface of the aqueous and organic phase of the emulsion, i.e. at the surface of the emulsion droplets (Langenberg, 2010; Galgali, 2011). The mechanism of MCs formation comprises four typical steps: (1) Formation of micro emulsion, (2) Initial polymerization at the interface, (3) Formation of membrane around the droplets, (4) Membrane growth to form the shell surrounding the isocyanate compound, or the matrix with the embedded isocyanate, free to react (Arshady, 1989; Duan, 2016; Latnikova, 2012). Figure 1, shows a schematic representation of microencapsulation by emulsion formation, followed by interfacial polymerization and related chemical reactions to form different types of shells. Several factors can affect the size, morphology and microencapsulation efficiency. These factors can be divided in two principal groups: i) factors related to primary material; ii) factors related to synthesis parameters. Surfactants, as one of the most important elements in the emulsion formation can affect emulsion stability, as well as MCs size, in the sense that higher surfactant concentration as MCs size, in the sense that higher surfactant concentration reduces the droplet size and narrows down the MCs size distribution (Duan, 2016; Yang, 2011). The chemical structure of the organic phase (isocyanate compound) can affect the porosity and permeability of the MC's shell (Duan, 2016). Higher functionality monomers and pre-polymers can improve the thermal and mechanical stability of MCs by formation of a three-dimensional cross-linked polymeric shell, leading to the formation of a less permeable shell (Duan, 2016). Solvents also, influence the capsules formation by changing the interfacial tension of the medium, which affects the contact area between isocyanate compounds and active hydrogen sources, leading to inhomogeneous reaction kinetics. Also, MCs´ diameter was found to decrease with an increase of the solvent's amount. An organic solvent can accelerate or decelerate the reactions by changing the diffusivity of the monomers towards their complementary phases. Moreover, the solvent evaporation during the drying stage also affects the MCs morphology (Duan, 2016; Polenz, 2014; Ma, 2017). Finally, chemical structure of active hydrogen source, its solubility in organic phase and aqueous phase (partition coefficient) and its concentration can strongly affect the morphology of the MCs, shell thickness and shell permeability (Polenz, 2014; Kardar, 2015; Ma, 2017; Tatiya, 2016). Chemical compounds with more NH or OH groups tend to produce a shell with a crosslinked network structure, leading to spherical MCs with thicker shell, while active hydrogen sources with linear structure and less active groups, result in thinner and softer shell structures (Tatiya, 2016). Synthesis physical conditions i.e. reaction temperature, emulsification rate and time and stirring rate can affect encapsulation efficiency, the size and size distribution of MCs, stability of emulsion and duration of reaction. Higher temperature during the synthesis can accelerate the formation of the shell by increasing the diffusion rate of monomers, as well as increasing the materials reactivity. It leads to a decrease of the MCs' core fraction, as well as denser and more thermally stable shells (Sun, 2015).

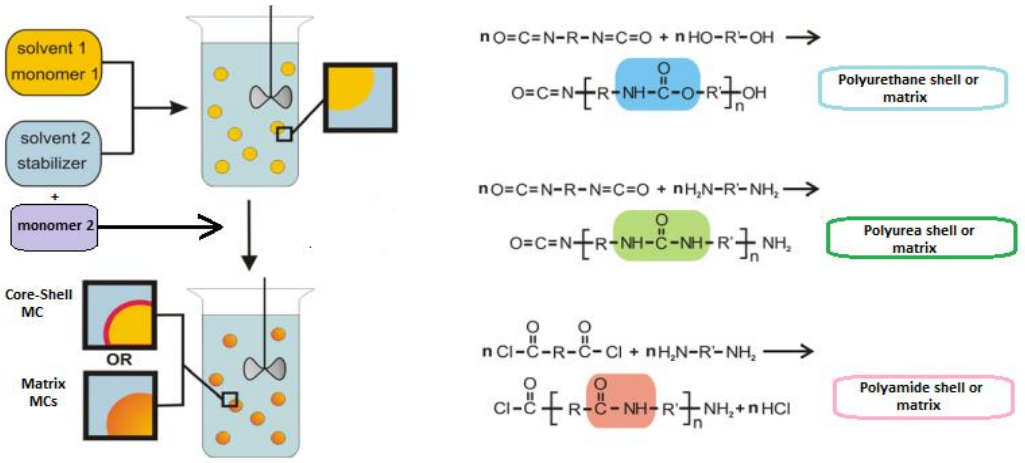


Figure 1. Schematic representation of microencapsulation by emulsion formation and interfacial polymerization (adapted from (Latnikova, 2012))

MCs diameter by increasing the emulsification rate (Zhuo, 2004; Tsuda, 2011). Moreover, the core fraction of MCs was found to decrease with an increase of the emulsification time (Sun, 2015). Several groups have studied the effect of the stirring rate in the MCs' size, thickness of the shell and the encapsulation yield (Brochu, 2012; Yang, 2011). Brochu et. al showed that, by increasing the stirring rate from 350 rpm to 1100 rpm, the average diameter of MCs decreased from 222 µm to 74 µm, the core content decreased from 58% to 46% and the shell thickness increased from 37 to 47%.

# 2 Experimental section

## 2.1 Materials

Toluene, n-hexane were supplied by VWR Chemicals, 2-Butanone (MEK) was supplied from Sigma-Aldrich, Ongronat 2500®, consisting of monomeric and polymeric species of isocyanate MDI, was supplied by BorsodChem. TDI was supplied from Dow, IPDI was supplied from Bayer, diethylenetriamine (DETA) was supplied by Alfa Aesar. Distilled water (W) MiliQ was obtained at the lab, Gum Arabic (GA) was supplied from LABCHEM, 1,6-Hexanediol and 3-(Triethoxysilyl) propyl isocyanate (TPI) were supplied from ALDRICH, 3-(2-aminoethylamino) propyltrimethoxysilane (aminosilane) was obtained from Dow Corning, Suprasec 2234, Desmodur® RC (MDI and TDI prepolymers, respectively) and PEARLSTICK® 45-50/18 (base component of the adhesive formulation, with an amount of OH groups) were kindly supplied from CIPADE S.A. All chemicals were used as received, without further purification.

## 2.2 Preparation of microcapsules

The MCs referred in this work were synthesized via microemulsion preparation, followed by interfacial polymerization. For the microemulsion preparation, two solutions, one corresponding to the aqueous phase (W) and the other to the oil phase (O) of the emulsion system, were mixed at 3200 rpm with an Ultra-Turrax (IKAT25 digital ULTRA TURRAX, Germany), resulting in the formation of a O/W emulsion system. The W phase solution was composed of deionized water and GA, while the organic phase was composed by a solution of isocyanate compounds in a certain solvent or without addition of any solvent. The emulsion was then transferred to a mechanical stirrer and stirred at 400 rpm. At this stage, another active hydrogen source was added (in some of the experiments) to the synthesis to form and modify the MCs' shell, through its reaction with the NCO groups of the isocyanate compound. This mixture was heated, by using a hot plate and the MCs obtained were filtrated with water, dried at room temperature (RT) and stored in a moisture free environment.

**2.2.1 Synthesis of MCs containing isophorone diisocyanate IPDI (IP-66 and IP-67)**

Microencapsulation of IPDI was carried out by the preparation of a mixture containing IPDI and Ongronat 2500® as the organic phase and 5 wt.% of GA in water, as the aqueous phase. The Ongronat 2500® was added to the IPDI in order to promote the MCs' shell formation, due to its higher reactivity. Upon emulsification, under mechanical stirring, an aqueous solution of DETA was added dropwise to the synthesis (IP-66). In other effort to encapsulate IPDI, TPI (Silane that contains double functionality: —NCO and—$OCH_2CH_3$. which are highly reactive) was added to the organic phase (IP-67). Both syntheses were stirred (400 rpm) during the 2 hr at 65-70° C.

**2.2.2 Synthesis of MCs containing Ongronat 2500® (IP-83 and IP-84)**

The procedure described in 2.1.1. was also applied to encapsulate Ongronat 2500® by addition of TDI to the organic phase of the emulsion system, which exhibits higher reactivity compared to Ongronat 2500®, promoting the shell formation. n-hexane was used as a solvent to dissolve TDI in Ongronat 2500®. For the synthesis IP-83, aminosilane was added dropwise to the emulsion, at 65 ℃ while, for the synthesis of IP-84, DETA, was the active hydrogen source added.to the emulsion. The emulsion then was stirred during the 3 hr at 400 rpm, with achievement of a mature shell.

**2.2.3 Synthesis of MCs containing Suprasec 2234 (IP-102)**

Due to the high reactivity of the prepolymer Suprasec 2234, several strategies were considered to control the reactions speed. In this paper, an example is given regarding encapsulation of Suprasec 2234, namely IP-102, where toluene was added to the organic phase as a solvent and DETA was employed as an active H source, following by mechanical stirring (300 rpm) at 55-60° C during the 1.5 hrs.

**2.2.4 Synthesis of MCs containing Desmodur RC (IP-118)**

The last series of synthesis was performed to encapsulate Desmodur RC as an isocyanate prepolymer(TDI). n-Hexane as a solvent and TPI was added to the organic phase of the emulsion system to form the shell (IP-118). The emulsion then was stirred (300 rpm) for an hour at 55-60 ℃ Moreover, several solvents were experimented to find out the proper solvent to dissolve this prepolymer.

## 2.3 Characterization

The adopted techniques and methods for the MCs characterization include: optical microscopy, scanning electron microscopy (SEM), Fourier transformed infrared spectroscopy (FTIR), thermogravimetric analysis (TGA) and peeling strength test.

**2.3.1 Optical microscopy**

Optical microscopy was performed to evaluate the emulsion condition during the synthesis and also to measure the MCs size and the occurrence of agglomeration after washing and drying the MCs. A Kruss, MSZ 5600 optical microscope and a Nikon microscope OPTIPHOT2-POL were used for this purpose.

**2.3.2 Scanning electron microscopy (SEM)**

The SEM characterization was performed using a JEOL 7001F (JEOL, Tokyo, Japan) SEM-FEG (field emission gun) microscope. Previously to the analysis, the MCs' samples were placed in a sample holder using a conductive adhesive tape with double face. Lastly, the samples were covered with a conductive thin film, by sputtering.

**2.3.3 Fourier transformed infrared spectroscopy (FTIR)**

The FTIR equipment used was a Nicolet 5700 FTIR (Thermo Electron Corporation, USA), equipped with a Smart iTR™ Attenuated Total Reflectance (ATR) sampling accessory. Spectra were measured at 8 $cm^{-1}$ resolution with a data collection of 16 scans.

**2.3.4 Thermogravimetric analysis (TGA)**

The analyses were performed in nitrogen controlled atmosphere, at a temperature

increase rate of 10 ℃ $min^{-1}$ using a TGA HITACHI STA 7200 equipment.

**2.3.5 Peeling strength test**

The peeling strength test was performed with the purpose of confirming the successful release of the MCs core content and its reaction with the surrounding environment (polyol based component, namely PEARLSTICK® 45-50/18, a base component of the adhesive formulation with an amount of OH groups), in response to certain stimuli, such as temperature and pressure. This test is critical to evaluate the adhesive effectiveness in the bonding process. There are three basic ways in which an adhesive bonded joint may fail: i) Cohesion failure, ii) Adhesion failure iii) Structural failure.

In cohesion failure, the failure is resultant from the fracture in the adhesive and is characterized by the clear presence of adhesive material on the matching faces of both adherents. Cohesion failure happens usually by shear, peel stresses or a combination of shear and peel stresses. Adhesion failures are characterised by the absence of adhesive material in one of the bonding surfaces and it is due to lack of the chemical or physical bonds which form the link between the adhesive and the surface. In the case of structural failure both adhesive and chemical or physical bonds between adhesive and substrate are strong enough and the failure will occur in the substrate. This is the target in this work. The type of failure that happens when selected MCs are employed was assessed in this work. In this test, a certain quantity of MCs was mixed with the polyol component (PEARLSTICK® 45-50/18). The mixture was then applied on the surface of paper by using an adjustable "Wet film thickness applicator". The test was performed under several physical conditions e.g. applying a certain temperature and/or load. A Thermaplate JAME H HELA was used to apply a certain temperature without any load, while a hot press CARVER, Model M, S/N 2000-3 62 was used to apply a certain load and temperature.

# 3 Results and discussion

## 3.1 MCs containing IPDI

Evaluation of MCs shape and morphology was carried out by optical microscopy and SEM. Figure 2 and 3 show the SEM photomicrographs of IP-66 and IP-67 respectively (MCs containing IPDI in their core).

Regarding synthesis IP-66, where DETA was added as an active hydrogen source, it is expected that its chain (longer than that of EDA), slows down its diffusion towards the organic phase (Zhang, 2009). Moreover, a more cross-linked polymer is generated during reaction of MDI with DETA, which also may enhance the stability of the emulsion. MCs from this synthesis were found to present a larger size (80-180 μm) and do not present any tendency to aggregate, due to addition of DETA. The high reactivity of DETA and the formation of a branched or cross-linked polymer, results in MCs with a thinner shell when compared with MCs to which other active hydrogen sources were added.

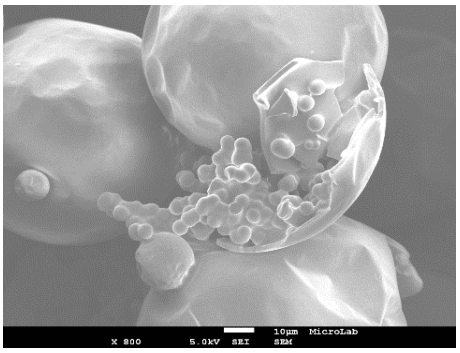


Figure 2. SEM photomicrograph of IP-66, Scalebar=10μm

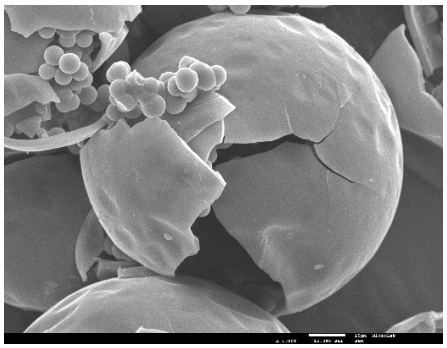

Figure 3. SEM photomicrograph of IP-67, Scalebar=10μm

Regarding synthesis IP-67, where TPI was added to the organic phase, it is expected that at the interface of the organic/aqueous phases of the emulsion, the alkoxide groups ($OCH_2CH_3$) from TPI suffer hydrolyzation, forming silanols, which will react with the NCO groups. On the other hand, the NCO groups from TPI will react with the OH groups from the aqueous phase. Also, the NCO groups from Ongronat 2500® prevalently tend to react with the aqueous phase, forming the shell material of the MCs. The MCs obtained in this synthesis also exhibit a spherical shape with a core-shell morphology and a thin shell, with some rough regions on the surface, probably due to the vacuum effect derived from the SEM operational procedure. Evaluation of these MCs by optical microscopy reveals a narrower range of size distribution, with the MCs' sizes varying between 50 and 90 µm. Also, by optical microscopy (Figure 4), it was possible to follow what happens when a MC (just before the filtration step) is broken with the help of a syringe needle: a significant amount of liquid isocyanate is released from the MC.

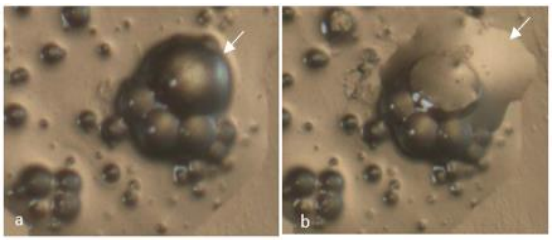


Figure 4. Optical microscopy image a) MCs before tearing of the shell with a needle, b) The same image after the break of the shell.

Figure 5 shows FTIR spectra, for MCs obtained from IP-66 and IP-67. It was possible to observe, for both MCs, an intense peak in the range of 2280-2260 $cm^{-1}$ related to the N=C=O stretch vibration bond, which reveals the presence of unreacted NCO groups in the MCs. There was also a peak at 1533 $cm^{-1}$ assigned to N-H bending, which can be derived from the presence of Ongronat 2500®, but also from the formation of urethane and urea linkages during the synthesis, which form the shell material. The sample prepared with DETA (IP-66), as expected, has a more intense peak at 1533 $cm^{-1}$. Also, there is a band peaked at ca. 1697 $cm^{-1}$ ascribed to the carbonyl groups of urethane and urea moieties, confirming that the formed shell is made of PU/PUa. On a first sight, further calculation was carried out to estimate a relative measure of the isocyanate encapsulation efficiency, by considering the peak area in the range of 1926 to 2444 $cm^{-1}$, for –NCO, the peak area in the range of 1754 to 1670 $cm^{-1}$, related to PU and/or PUa (carbonyl groups) and the peak area in the range of 1090 to 1026 $cm^{-1}$, for Si-O-Si. The peaks area was calculated using the OriginPro 8 software, and the "relative encapsulation yield", referred as Y throughout this paper, was calculated based on the equation below.

$$Y = \frac{Area_{NCO}}{Area_{PU+PUa}+Area_{siloxane}}$$

where Y represents a relative encapsulation efficiency and $Area_{NCO}$, $Area_{PU+PUa}$ and $Area_{Siloxane}$, represent the area related to the NCO, PU+PUa and siloxane related peaks, respectively.

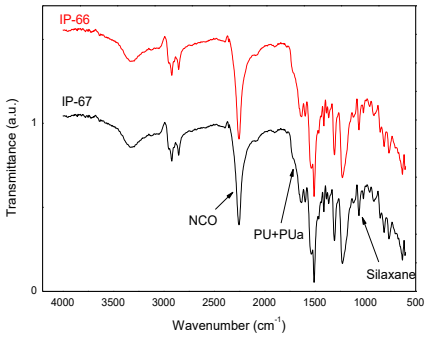


Figure 5. FTIR for IP-66 and IP-67 and identification of the peaks used for calculation of the areas related with NCO, PU+PUa and Siloxane.

By using the mentioned equation, a Y=43.20 and a Y=41.40 were obtained for IP-66 and IP-67 respectively, which reveal a quite similar isocyanate encapsulation.

TGA analyses show a weight loss behaviour that happens in several general steps. The first step comprises water and other solvents evaporation, the second step is defined by the decomposition of encapsulated isocyanate and the last step is related with the MCs' polymeric shell decomposition, which can be divided in two steps: decomposition of soft segments (derived from active hydrogen source) and

decomposition of hard segments. It should be stressed that there is an overlap resulting from the decomposition of isocyanate compounds (monomers and pre-polymers) and PU and PUa material, so there is not exactly any border line to separate them. There are references which mention that PU decomposition starts around 200˚C (Brochu, 2012), however the decomposition of isocyanates is also around this temperature (Yang, 2008; Li, 2011; Yi, 2012). Also, it should be noted that the decomposition temperature range for encapsulated isocyanate compounds is slightly different from that of non-encapsulated ones, and such difference will depend on the MCs´shell thickness, composition and structure (Brochu, 2012; Koh, 2014). Being so, it was possible to obtain a core mass of 24 wt% and 51 wt% for IP-66 and IP-67 respectively (thermograms not shown in this paper).

### 3.2 MCs containing Ongronat 2500®

Figures 6 and 7 show the SEM photomicrographs of IP-83 and IP-84.

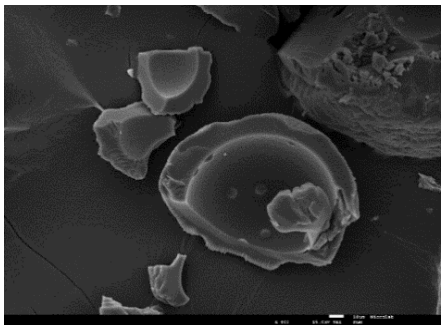

Figure 6. SEM photomicrograph of IP-83, Scalebar=10µm

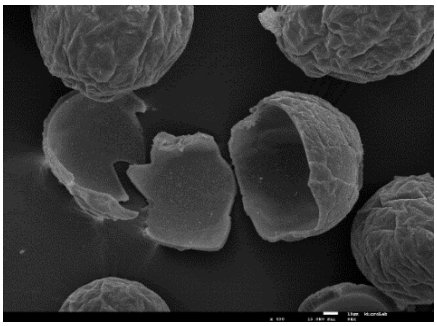

Figure 7. SEM photomicrograph of IP-84, Scalebar=10µm

MCs from IP-83 (Figure 6), with aminosilane as active hydrogen source, have mostly a spherical shape, with no tendency to aggregate. The size distribution of the MCs is in the range of 70-200 µm, as it is observed from SEM photomicrographs, and the internal surface of the MC's shell looks smooth. This fact can be due to the employment of n-Hexane as a solvent which might change the solubility of the amine in the oil phase. Aminosilane, when incorporated into the aqueous phase tends to hydrolyse, forming silanol groups. Also, the amino groups tend to react with the NCO groups at the interface of the aqueous/organic phases. The silanol groups, on the other hand, by polycondensation reactions, form siloxane moieties (FTIR peak assignment at ca. 1100 $cm^{-1}$), improving the mechanical strength and thermal resistance of the resulting shell, which will be a hybrid material based on PU/PUa and silica.

Figure 7 shows the SEM photomicrograph of MCs from IP-84, made with DETA, which are found to have thinner shells than those from IP-83, maybe because DETA tends to react faster and the shell achieves maturity sooner. The difference in the surface morphology of the MCs shell, can be justified by differences in the partition coefficient ($K_{OW}$) for aminosilane and DETA.

The same calculation used from FTIR results reveals Y=5.47 and Y=86.17 for IP-83 and IP-84, respectively, which shows that DETA leads to a better result in terms of encapsulation yield. This result is corroborated by TGA, which shows that the core mass for IP-83 is 12 wt% and for IP-84 is 26 wt% (thermograms not shown in this paper).

### 3.3 MCs containing Suprasec 2234

Figure 8 shows SEM photomicrograph of MCs obtained from IP-102, where DETA was added dropwise to the synthesis to form the MCs' shell. The MCs have diameters in the range of 10 to 100 µm with some aggregation and exhibit a rough surface, which can be justified by an inhomogeneous reaction kinetics (Kardar, 2015; Tatiya, 2016). The FTIR analysis confirmed a successful encapsulation of Suprasec 2234 with Y=4.05.

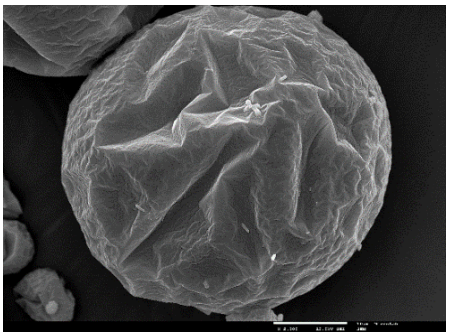

Figure 8. SEM photomicrograph of IP-102, Scalebar=10µm

### 3.4 Microcapsules containing Desmodur RC

The best results in this series of synthesis was obtained for IP-118 by addition of TPI as a cross linker and n-Hexane as a solvent to the organic phase. FTIR analysis has confirmed successful encapsulation of Desmodur RC with Y=5.7.

### 3.5 Synthesis parameters study and optimal microencapsulation procedure

Several studies were carried out based on the synthesis for encapsulation of IPDI to obtain an optimal microencapsulation procedure. These studies revealed that:

i) A higher amount of GA leads to smaller size droplets. On the other hand, the stability of the emulsion and the shape of the droplets did not show any significant changes for different concentrations of GA, ranging from 2wt% to 22wt%;

ii) By increasing the emulsification rate from 3200 rpm to 9000 rpm the size of the droplets changed from (35-270µm) to (6-70µm), revealing to be a good approach to tune the size of the MCs. Tsuda et al. have reported the same behaviour (Tsuda, 2011);

iii) By increasing the temperature of the synthesis, its duration tends to decrease. This can be explained by a higher reaction rate. The temperature range of 70-75°C was found to be the best range to obtain the highest encapsulation yield.

### 3.6 Peeling strength test

MCs obtained from IP-84 and IP-118 were the ones selected for peeling strength tests. 5wt% of MCs were added to a solution of 25 wt% PEARLSTICK® 45-50/18 in MEK. The tests were carried out in three conditions: i) by applying a temperature of 80ºC; ii) by applying a pressure of 4 $kg.cm^{-2}$; iii) by applying both temperature and pressure simultaneously. As a result, it was found that both MCs show adhesive failure when applying just temperature to the test, and structural failure of the adhesive joint when applying load or load and temperature (Figure 9). In fact, it was not expected that the effect of temperature, as by itself, enough to lead to the isocyanate release from the MCs, however the application of a pressure at 4 $Kg.cm^{-2}$ was enough to break the MCs, leading to a structural failure in the peeling strength test, which is the type of failure that denotes a stronger adhesion of the substrate, and, therefore, an effective performance of the MCs.

Figure 9. Structural failure, IP-84

## 4 Conclusions

In this work it was developed an approach, which deals with the combination of low and high reactivity isocyanate compounds, to provide a more efficient encapsulation. Having this in mind, it was possible to encapsulate four different types of isocyanate compounds, including isocyanate prepolymers which are highly reactive commercial crosslinkers for adhesive formulations. The adhesion performance, when using selected MCs, was assessed through peeling strength tests and analysis of the failure type of the adhesive joints. It was found that the MCs provide an efficient adhesion performance when blended with the base compound of the adhesive formulation (that contains a certain amount of OH groups), denoted by the structural failure type achieved.

From all the laboratory experiences, it was possible to conclude, for each isocyanate compound, about the best combination in terms of active hydrogen source and solvent employed, which is listed in Table 1.

Table 1-The best combination of active hydrogen source and solvent for each isocyanate compound in this work

| Isocyanate compound | Active hydrogen source | Solvent |
|---|---|---|
| IPDI | DETA | None |
| Ongronat | DETA | n-Hexane |
| Suprasec 2234 | DETA | Toluene |
| Desmodur RC | TPI | n-Hexane |

GA was a good performing surfactant in this work. Higher concentration of GA resulted in a decreasing of the MCs size. A temperature range of 75-77 ℃ was found to improve the encapsulation efficiency, by reducing the synthesis duration. As an example, in the case of Suprasec 2234 and Desmodur RC, the decrease of synthesis temperature from 60 ℃ to RT, implied an increase of the synthesis' duration from 20 minutes to 4 hours, while a decrease in temperature, by using an ice bath, has stopped the reaction.

Although the lower stirring rate improves the encapsulation efficiency, it was found to increase the synthesis duration, so the range from 350 to 400 rpm can be considered as the best practical range.

An increase in the emulsification rate was found to lead to a decrease in the MCs size.

## 5 Future work

Development of MCs with more brittle shell, so they can fully release the isocyanate by the effect of loading (pressure): a few experiments have been done to synthesize MCs with brittle shells by addition of PS solution in several solvents i.e. toluene, DCM, MEK, etc. Although the FTIR spectra of MCs confirmed the presence of PS, there are still some efforts necessary to optimize these syntheses.

Development of MCs with thermal gates, so they can fully release the isocyanate by melting: a few experiments were carried out to synthesize MCs with thermal gates by adding to the synthesis a solution of PCL in different solvents, however, more efforts in this field should be done.

Test of new promising active hydrogen sources, to improve the encapsulation efficiency of Suprasec 2234 and Desmodur RC: 1,4 Butanediol, TETA and 0.0 G PAMAM might be tested.

Some of the MCs containing Suprasec and Desmodur were not possible to be broken by the tip of a needle. In this case, embedding them in resin as a mounting material, following by cutting the mounted sample by micro cutter might be done, to better study their morphology and check if they have a core-shell morphology, or not.

## References


R. Arshady, (1998). Preparation of microspheres and microcapsules by interfacial polycondensation techniques. *Journal of microencapsulation*, Vol.6, 13-28. doi:10.3109/02652048909019898

A.B. Brochu, W. J. Chyan, W.M. Reichert, (2012). Microencapsulation of 2-octylcyanoacrylate tissue adhesive for self-healing acrylic bone cement. *Journal of Biomedical Materials Research - Part B Applied Biomaterials*, Vol.100, 1764-1772. doi:10.1002/jbm.b.32743 B.

Duan, (2016). Microencapsulation via In Situ Polymerization. In *Handbook of Encapsulation and Controlled Release* by D.R. Karsa and R.A. Stephenson Published by Woodhead Publishing Limited.

ECOBOND. (2015). Portugal 2020 Co-Promotion Project # 17930. "Development of new ecological, self-reactive, monocomponent adhesives". Portugal.

G. Galgali, E. Schlangen, S. V. D. Zwaag, (2011). Synthesis and characterization of silica microcapsules using a sustainable solvent system template. (Elsevier, Ed.) *Materials Research Bulletin,* Vol.46, 2445-2449. doi: 10.1016/j.materresbull.2011.08.028.

P. Kardar, (2015). Preparation of polyurethane microcapsules with different polyols component for encapsulation of isophorone diisocyanate healing agent. *Progress in Organic Coatings*, Vol.89 271-276. doi: 10.1016/j.porgcoat.2015.09.009.

E. Koh, N. K. Kim, J. Shin and Y.W. Kim, (2014). Polyurethane Microcapsules for Self-Healing Paint Coatings. *RSC Advances*, Vol.*4, 15830-15834,* http://dx.doi.org/10.1039/C3RA41454J

K. V. Langenberg, P. Warden, C. Adam and H.R. Milner (2010). The durability of isocyanate-based adhesives under service in Australian conditions (Literature Review). *Forest & Wood Products Australia Limited.*

A. Latnikova, (2012). Polymeric capsules for self-healing anticorrosion coatings. PhD dissertation in physical chemistry. Faculty of mathematics and natural sciences, *the University of Potsdam*.Germany.

L. Zhuo, C. Shuilin and Z. Shizhou, (2004). Factors affecting the particle size and size distribution of polyurea microcapsules by interfacial polymerization. *International Journal of Polymeric Materials and Polymeric Biomaterials*, Vol.53, 7-41. doi:10.1080/00914037108071852.

Y. Ma, Y. Jiang, H. Tan, Y. Zhang and J. Gu, (2017). A Rapid and Efficient Route to Preparation of Isocyanate Microcapsules. *Polymers*, Vol.7, 24-27. doi:10.3390/polym9070274.

J. Nikkola, (2014). Microcapsule-protected actives reduce leaching. *European Coatings Journal*, Vol.4, 36-40.

I.Polenz, S.S. Datta and D.A, Weitz, (2014). Controlling the morphology of polyurea microcapsules using microfluidics. *Langmuir*, Vol.44, 13405-13410, DOI: 10.1021/la503234z.

D. Sun, J. An, G. Wu and J. Yang. (2015). Double-layered reactive microcapsules with excellent thermal and non-polar solvent resistance for self-healing coatings. *Journal of Materials Chemistry A*, Vol.3, 4435-4444. doi:10.1039/c4ta05339g

T.F. Tadros, (2013). Emulsion Formation, Stability, and Rheology, pp. 1-75, Wiley-VCH Verlag GmbH & Co. KGaA. doi: 10.1002/9783527647941.ch1.

P. D. Tatiya, R. K Hedaoo, P. P. Mahulikar, and V. V. Gite, (2016). Designing of polyamidoamine-based polyurea microcapsules containing tung oil for anticorrosive coating applications. *Journal of Coatings Technology and Research*. Vol.13, 715-726, doi:10.1007/s11998-015-9780-2.

M. Huang and J. Yang, (2011). Facile microencapsulation of HDI for self-healing anticorrosion coatings. *Journal of Materials Chemistry*, Vol.48, 24959- 25506, doi:10.1039/c1jm10794a.

Yang, M. H. (2011). Facile microencapsulation of HDI for self-healing anticorrosion coatings. *Journal of Materials Chemistry*, 11123. doi:10.1039/c1jm10794a.

H. Zhang, X. Wang, (2009). Synthesis and properties of microencapsulated n-octadecane with polyurea shells containing different soft segments for heat energy storage and thermal regulation. *Solar Energy Materials and Solar Cells*, Vol.93, 1366-1376. doi: 10.1016/j.solmat.2009.02.021.